PID controlling approach based on FBG array measurements for laser ablation of pancreatic tissues

Sanzhar Korganbayev, Annalisa Orrico, Leonardo Bianchi, Davide Paloschi, Alexey Wolf, Alexander Dostovalov, and Paola Saccomandi.

***Abstract*—In this paper, we propose a temperature-based proportional–integral–derivative (PID) controlling algorithm using highly dense fiber Bragg grating (FBG) arrays for laser ablation (LA) of *ex vivo* pancreatic tissues. Custom-made highly dense FBG arrays with a spatial resolution of 1.2 mm were fabricated with the femtosecond point-by-point writing technology and optimized for LA applications. In order to obtain proper PID gain values, finite element method-based iterative simulation of different PID gains was performed. Then, the proposed algorithm, with numerically derived PID gains, was experimentally validated. In the experiments, the point temperature was controlled at different distances from the laser fiber tip (6.0 mm, 7.2 mm, 8.4 mm, and 10.8 mm). The obtained results report robust controlling and correlation between controlled distance and the resulting area of ablation. The results of the work encourage further investigation of FBG array application for LA control.**

***Index Terms*— closed-loop temperature control, fiber Bragg grating sensors, feedback system, optical fiber, PID control, temperature monitoring, thermal ablation, pancreas.**

I. Introduction

Pancreatic ductal adenocarcinoma (PDAC) is the fourth cause of cancer deaths in the world, with about 57,600 new cases and 47,050 deaths in 2020 in the United States only [1]. This number is estimated to increase, and by 2030 PDAC will become the second leading cause of cancer-related death [2]. The main reasons for such statistics are difficulty in early diagnosis, high biological aggressiveness, and inefficiency of traditional approaches. Recently, thermal ablation (TA) techniques have received increasing interest in PDAC treatment due to their minimal invasiveness [3]. The main principle of these techniques is based on inducing local temperature change that leads to tumor necrosis. Depending on the source of temperature change, different ablation types exist: radiofrequency, microwave, ultrasound, and laser ablation (LA) [4].

Among all ablation techniques, LA has unique advantages such as flexibility and electromagnetic immunity of the fiber optic applicator, which allow the treatment of deep-lying organs under image guidance [5]. LA is based on the laser light absorption and scattering inside ablated tissue, which leads to temperature elevation and, consequently, to thermal damage of the treated tumor. For deep tumors, laser wavelengths in the so-called "therapeutic window" (940 nm –1100 nm) are mostly utilized due to a good tradeoff between penetration depth and absorption of laser light by the tissue that entails the possibility to ablate large areas (tens of millimeters) [6].

However, the main limitation of LA, as well as other ablation techniques, is an uncertainty of the treatment results due to the complexity of the ablation phenomenon and the heat-tissue interactions [7], [8].

One of the possible solutions is a minimization of the uncertainty of the procedure by introducing a closed-loop approach based on measurements of intra-tissue parameters in the ablated region. One of the most important parameters to evaluate the efficacy of TA is temperature. Different ranges of temperatures have different effects on biological tissues. Temperatures from 42 °C to 45 °C correspond to hyperthermia and related activation of an immune response. At temperatures from 50 °C to 55 °C, coagulative necrosis of organs and instantaneous death in cell culture can be observed [7], whereas 60 °C is the starting temperature for rapid denaturation. As a result, accurate control of the desired temperature range is an important factor to ensure efficient cancer treatment.

It is worth noting that not only the tissue temperature value but also the time the tissue is exposed to this value are important to properly evaluate the thermal effect [8]. Thus, different

Manuscript received XXX; revised XXX; accepted XXX. Date of publication XXX; date of current version XXX.

This project has received funding from the European Research Council (ERC) under the European Union's Horizon 2020 research and innovation programme (Grant agreement No. 759159). The work of A.W. and A.D. is supported by the Russian Ministry of Science and Higher Education (Grant No. 14.Y26.31.0017)

Sanzhar Korganbayev, Annalisa Orrico, Leonardo Bianchi, Davide Paloschi, and Paola Saccomandi are with the Department of Mechanical Engineering, Politecnico di Milano, 20156 Milan, Italy (e-mail: sanzhar.korganbayev@polimi.it; annalisa.orrico@polimi.it; leonardo.bianchi @polimi.it; davide.paloschi@polimi.it; paola.saccomandi@polimi.it).

Alexey Wolf and Alexander Dostovalov are with Department of Physics, Novosibirsk State University, 630090 Novosibirsk, Russia, and also with the Institute of Automation and Electrometry, Siberian Branch of the Russian Academy of Sciences, 630090 Novosibirsk, Russia (e-mail: wolf@iae.nsk.su; dostovalov@iae.nsk.su).

models have been proposed to assess the thermal damage of TA techniques considering both these aspects. One of the models is the Cumulative Equivalent Minutes at 43 °C (CEM43), which has been used to assess the severity of thermal damage for several tissue types [9]. In this regard, as will be discussed later in the paper, the proposed LA regulation maintains controlling temperature at 43 °C during LA experiments.

The state-of-the-art works on temperature-based LA control mostly utilize traditional types of sensors: thermocouples [10], [11], and thermistor probes [12], [13]. The main disadvantages of these methods are the metallic material of the sensors and their low spatial resolution. Metallic material absorbs laser light and heat; thus, leading to overestimation of temperature that can reach above 20 °C [14], [15]. The low spatial resolution of conventional sensors does not allow proper temperature reconstruction due to high thermal gradients, especially in the proximity of the applicator tip [8].

One of the possible alternatives to thermocouples and thermistors is the use of fiber Bragg grating (FBG) sensors. FBGs, as most optical sensors, are immune to electromagnetic interference, are small in size, and biocompatible. These advantages have led to increasing interest in FBG applications in LA treatments [16], [17].

Recently, our group has been working on FBG array applications for LA regulation using the ON-OFF controlling approach. The aim was the regulation of maximum temperature [18] and zone control [19] during contactless LA, and temperature control at different distances from the laser fiber tip during interstitial LA [20] of liver tissues. In order to improve controlling performance, in this paper, we propose and experimentally validate a PID-based approach applied to the interstitial ablation of pancreatic tissue. In addition, the model of the heat transfer inside the tissue undergoing LA has been used for optimizing the choice of the PID parameters to be used in the experiments.

II. Materials and Methods

A. FBG array sensors

FBG is a periodic modulation of refractive index in the fiber core that behaves as a wavelength-dependent reflector, transmitting all wavelengths except the characteristic Bragg wavelength λ_B. The Bragg wavelength is proportional to the periodicity of modulation Λ:

$$\lambda_B = 2n_{eff}\Lambda \quad (1)$$

where n_{eff} is the effective refractive index of the core mode field.

The working principle of FBG relies on the fact that a temperature change ΔT alters Λ and n_{eff}, and, as a result, λ_B [21]:

$$\frac{\Delta\lambda_B}{\lambda_B} = \alpha \cdot \Delta T \quad (2)$$

where α ($^{\circ}C^{-1}$) is the thermal sensitivity of the grating and $\Delta\lambda_B$ is the variation of λ_B.

Therefore, it is possible to reconstruct temperature changes along the FBG by measuring the $\Delta\lambda_B$ values. In addition, an array of FBGs along the fiber (each FBG with different Λ and λ_B) can provide quasi-distributed temperature measurements, where each FBG acts as a sensing point.

Custom-made highly dense FBG array used in the experimements was fabricated with femtosecond point-by-point writing technology. The FBG array was inscribed in polyimide-coated single-mode fiber SM1500(9/125)P (Fibercore Ltd., Southampton, UK) with a reduced coating diameter (~145 μm). For femtosecond point-by-point inscription, Pharos 6W (Light Conversion, Vilnius, Lithuania) femtosecond laser system producing pulses with a wavelength of 1026 nm and duration of 232 fs was utilized. ABL1000 (Aerotech Inc, Pittsburgh, PA, USA) air-bearing linear stage was used for high-precision pulling of the fiber through the glass ferrule to set the position and individual resonant wavelength for each FBG in the array.

Pulling of the fiber with the predefined velocity ($v_i \sim 1$ mm/s) and simultaneous femtosecond irradiation with laser pulse sequence (f = 1 kHz) results in FBG inscription. The obtained Bragg wavelength is defined by $\lambda_{B,i} = 2n_{eff}\Lambda_i = 2n_{eff}v_i/mf$, where $m = 2$ is an order of FBG.

All 40 FBGs in the array were uniformly distributed in the spectral range of the used interrogator (1460-1620 nm) in order to reduce mutual interference of the neighboring gratings. Each of the gratings had a length of 1.15 mm, an edge-to-edge distance of 0.05 mm (the total length of the FBG array is 48 mm), and a uniform refractive index modulation profile, which gave us an FWHM spectral width of the grating of ~700 pm. The reflection coefficient of an FBG in the range of 10-20% allowed us to record the array reflection spectrum with a high dynamic range (> 30 dB).

These FBG properties were optimized to have a narrow Bragg spectral width and at the same time to ensure accurate measurements of high-gradient temperature profiles that can reach up to 50 °C/mm near the applicator during LA procedures [8]. Moreover, the polyimide coating of the arrays provides the high thermal resistance (up to 400 °C) needed for accurate quasi-distributed measurements in this application [22]–[24]. The temperature sensitivity of the arrays is $(7.43 \pm 0.01)\times10^{-6}$ $^{\circ}C^{-1}$. More information about the fabrication and the metrological characterization of the sensors can be found in the previous works of the group [19], [24].

The Micron Optics si255 optical interrogator (Micron Optics, Atlanta, USA, 1 pm accuracy, wavelength range 1460 nm-1620 nm) was utilized to measure the reflected spectra from the FBG arrays with a 100 Hz sampling rate.

B. Laser ablation equipment

Interstitial LA experiments were performed on *ex vivo* healthy porcine pancreatic tissue, which was obtained from a local farm. After the removal, the organs have been immediately placed in a sealed bag and stored in the fridge (4 °C). For the experiments, each specimen was prepared with a size suitable for placing in the custom-made box, which were used for accurate positioning of the sensor and laser fiber. The tissue

temperature before the start of experiments was maintained at room temperature equal to 22 °C.

The diode laser (LuOcean Mini 4, *Lumics*, Berlin, Germany) working in continuous-wave mode at a 1064 nm wavelength was used for ablation. This wavelength belongs to the "therapeutic window" largely used for assuring the overall absorption of the laser light by the biological tissues, thus, to entail the temperature increase necessary for the thermal therapy. It is worth noticing that 1064 nm is the wavelength that has been used for the first human trial on pancreatic tumors [25]. The flexible quartz optical fiber (300 µm diameter) was used to guide laser light inside the tissue.

The laser diode driver allows changing the output optical power via electrical current modulation during laser irradiation. For PID controlling, an electrical current range of 3000 mA (minimal current of the laser diode) - 8000 mA was chosen. In order to obtain corresponding power values, power was measured with a Newport 843-R-USB power meter (*Newport Corporation*, Irvine, USA) for the current range selected. As a result, the obtained power range used for the PID temperature regulation experiments was 1.8 W – 6.6 W.

C. Experimental Arrangement

The developed system consists of the laser diode and the Micron Optics interrogator, both connected to a computer where a custom-made LabVIEW program was used to regulate LA.

A custom-made plexiglass box was employed to guarantee the accurate positioning of the laser fiber and sensors. The holes located on all sides of the box allow for different sensor and applicator arrangements in the tissue (Fig. 1).

The fibers were placed with the help of medical needles to prevent their damage during insertion into the pancreatic tissue. Initially, an 18-gauge needle (5 cm length) was inserted in the central hole of the lateral face of the box, and a 21-gauge needle (11 cm length) was inserted in a different hole at a 6 mm distance from the central one. Subsequently, the laser fiber and the FBG array fibers were inserted into the needles. The needles were then pulled out so that only the fibers remained inside the tissue.

The initial temperature of the pancreas, corresponding to 22.0 ± 0.5 °C, was measured with a thermocouple before each experiment. After experiments, the ablated volume was cut in the middle, and the axes of the ablated region were measured.

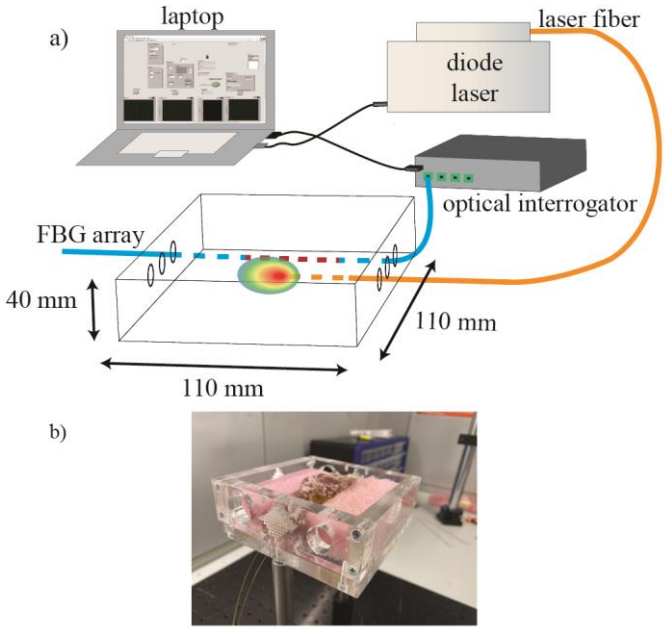

Fig. 1. (a) Schematics of the experimental setup: laser fiber and FBG array inserted in pancreatic tissue positioned in custom-made box; LA regulation setup consists of optical interrogator, diode laser, and laptop; (b) photo of sensors and laser fiber positioned in pancreatic tissue.

D. Controlling algorithm

The developed LabVIEW program has two main phases (Fig. 2):

(a) the input of preset parameters: set temperature T_{set}, PID gains, and *d* (distance between the grating with maximum temperature and the controlled grating);

(b) start of ablation with constant power (3.3 W) until a threshold of 10 °C of temperature change is reached. Then, the position of the grating exposed to the maximum temperature (FBG_{max}) is saved and position of the controlled grating (FBG_{con}) is calculated using *d* value. After, regulation of the controlled temperature (T_{con}) at the controlled grating (FBG_{con}) is performed using the PID approach. Finally, after 300 s of steady-state time (t_{ss}), the laser is switched off.

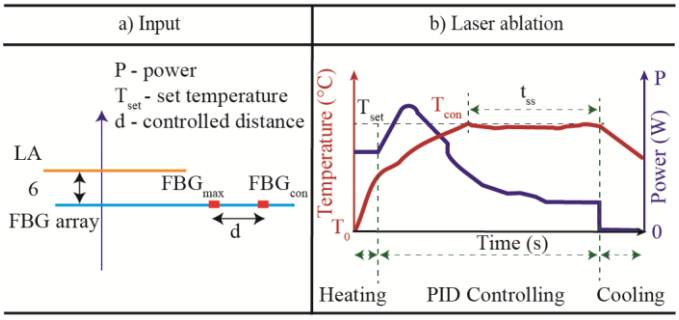

Fig. 2. Schematics of laser ablation algorithm; (a) set of input parameters; (b) schematics of controlled temperature evolution and related power during LA.

E. Pre-planning Model

In order to have an initial estimation of the gain coefficients of the PID controller, the heat-transfer phenomenon caused by

the interaction between laser and the pancreas was simulated, along with the effects of the PID control.

The temperature distribution of an *ex vivo* biological tissue subjected to laser-induced thermal treatment is governed by the bio-heat transfer equation [26], expressed as:

$$\rho \cdot c \cdot \frac{\partial T(t,r,z)}{\partial t} + \nabla(-k\nabla T(t,r,z)) = Q_{source} \quad (3)$$

where T(t,r,z) (K) is the tissue temperature, while the density, the specific heat, and the thermal conductivity of the biological tissue are represented with ρ ($kg \cdot m^{-3}$), c ($J \cdot kg^{-1}K^{-1}$), and k ($W \cdot m^{-1}K^{-1}$) respectively; the term Q_{source} ($W \cdot m^{-3}$) represents the deposited thermal energy delivered by the laser source. Since the latter term is strongly affected by the light propagation in the tissue, a simple diffusion approximation method was employed to correctly predict the deposited thermal energy. The Beer-Lambert law [27] was used to predict the light propagation inside the tissue:

$$\frac{\partial I(t,r,z)}{\partial z} = -\alpha_{eff} \cdot I(t,r,z) \quad (4)$$

The resulting deposited thermal energy [28] can be expressed as:

$$Q_{laser} = \alpha_{eff} \cdot I_0(t,r) \cdot e^{-\alpha_{eff} \cdot z} \quad (5)$$

where z (m) is the axial depth in tissue and α_{eff} (m^{-1}) is the effective attenuation coefficient that was calculated based upon diffusion approximation [29] to consider both the absorption and the scattering phenomena. Lastly, I_0 ($W \cdot m^{-2}$) represents the laser irradiance and is expressed as:

$$I_0(t,r) = \frac{P(t)}{2\pi\sigma^2} \cdot e^{-\frac{r^2}{2\sigma^2}} \quad (6)$$

where σ (m) is the standard deviation related to the beam profile, r (m) is the radial distance, and P (W) is the laser power that is linearly dependent on the laser current C (A). This last parameter is set by a PID controller as follows:

$$C(t) = k_p \cdot (T_{set} - T_{con}) + k_i \cdot \int_0^t (T_{set} - T_{con}(\tau))d\tau + k_d \cdot \frac{d(T_{set} - T_{con}(t))}{dt} \quad (7)$$

The PID controller maintains the temperature T_{con} (K) at the same value of the setpoint temperature T_{set} (K), upon a proper selection of the proportional k_p ($A \cdot K^{-1}$), integral k_i ($A \cdot K^{-1} \cdot s^{-1}$) and derivative k_d ($A \cdot s \cdot K^{-1}$) gain coefficients.

III. Results and Discussion

A. Pre-planning of PID gains

The numerical model of the interstitial LA was solved using the finite element method (FEM)-based solver: COMSOL Multiphysics (COMSOL, Inc., Burlington, MA, USA). Several simulations were run to assess the best set of parameters for the PID controller based on the tissue thermal response. The tested gain coefficients are reported in Table I, and corresponding temperature profiles are reported in Fig. 3a.

TABLE I
PID GAINS FOR DIFFERENT SIMULATION SETS

	k_p ($A \cdot K^{-1}$)	k_i ($A \cdot K^{-1} \cdot s^{-1}$)	k_d ($A \cdot s \cdot K^{-1}$)
Set 1	10	1	0
Set 2	1	10	5
Set 3	0.1	0.6	0
Set 4	0.7	0.006	0
Set 5	0.7	0	20

Fig. 3 shows the simulated thermal responses and the related output power profiles needed to achieve the setpoint temperature of 43 °C under five different PID settings at *d* = 10.8 mm. The output power profiles of Set 1, Set 2, and Set 3 experience abrupt changes when the controlled temperature approaches the setpoint value (Fig. 3b). These PID sets do not possess control moderation and use mainly the minimum and maximum power available; consequently, they are not able to react in advance to the heat diffusion generated by a thermal gradient. As a result, they experience temperature overshoots and very lethargic setpoint tracking due to the suboptimal choice of the gains (Fig. 3a).

The light blue curve denotes the thermal response of the tissue temperature in the absence of the integral term in the PID system. Since k_i is responsible for enforcing zero steady-state error [30], the steady-state response of Set 5 is not able to reach the setpoint temperature. Conversely, the gain parameters selected in the Set 4, i.e., $k_p = 0.7$ $A \cdot K^{-1}$, $k_i = 0.006$ $A \cdot K^{-1} \cdot s^{-1}$ and $k_d = 0$ $A \cdot s \cdot K^{-1}$ showed a smoother power profile and a thermal response characterized by a rise time of ~ 350 s and a smaller temperature overshoot of ~ 1.8 °C (Fig. 3, green line). These last PID gain parameters were used for the experiments.

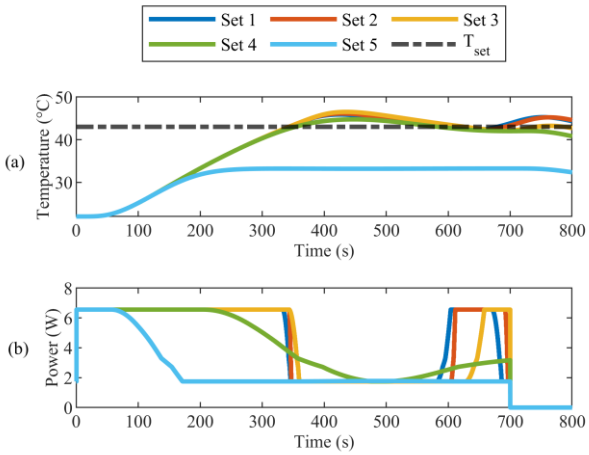

Fig. 3. Simulated temperature (a) and laser power (b) profiles for the different sets of PID gain values.

Robustness of selected PID gains for different controlled distances was checked by changing the position of the controlled point from *d* = 10.8 mm to *d* = 7.2 mm. Fig. 4 reports that the selected gains allow to have a good controlling

This article has been accepted for publication in a future issue of this journal, but has not been fully edited. Content may change prior to final publication. Citation information: DOI 10.1109/TIM.2021.3112790, IEEE Transactions on Instrumentation and Measurement

performance (*i.e.*, rising time of ~ 350 s and a temperature overshoot of ~ 0.5 °C) also for d = 7.2 mm.

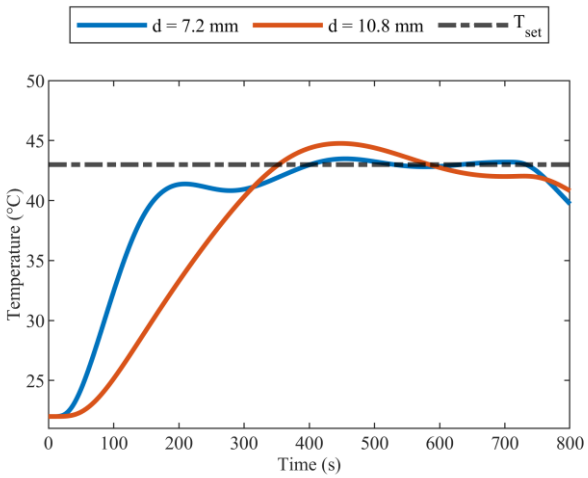

Fig. 4. Simulated controlled temperature profiles for different controlled distances.

Fig. 5 illustrates the temperature distributions resulting from the LA regulation shown in Fig. 4 for d = 10.8 mm (Fig. 5 left side) and d = 7.2 mm (right side). Different thresholds were selected to display the volumes of pancreatic tissue subjected to specific temperatures, relevant for laser-assisted treatment purposes, in particular: *(i)* sublethal damage around T ~ 43 °C, *(ii)* instantaneous thermal damage for T ≥ 60 °C, *(iii)* vapor diffusion and tissue desiccation at T ≥ 100 °C, *(iv)* removal of tissue mass for T ≥ 300 °C [31]. As can be seen from Fig. 5, the controlled distance d affects the temperature distribution and, therefore, the extension of the thermal damage.

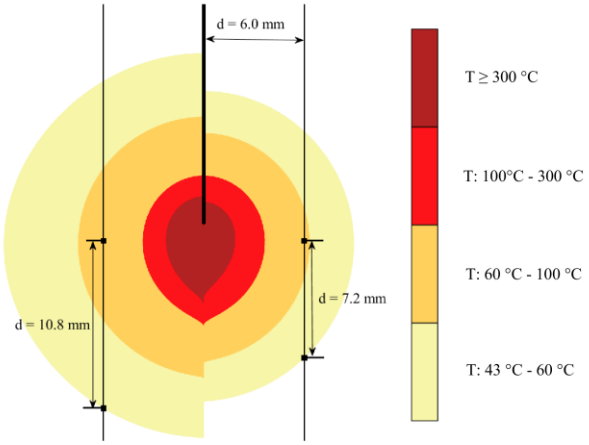

Fig. 5. Simulated temperature distributions for controlled distance equal to d = 10.8 mm (left) and d = 7.2 mm (right).

B. *Experimental Results*

After pre-planning the PID controller and obtainment of the gain values, we used them for the experimental tests. In particular, experiments with different d values (d = 6.0 mm, 7.2 mm, 8.4 mm, and 10.8 mm) were performed to further assess the robustness of the control strategy towards different distances and to validate the proposed LA regulation approach.

Fig. 6 reports the evolution of the controlled temperature and the laser power during LA of the pancreas. As it can be seen, the controlling algorithm allows for the proper regulation of the set temperature T_{set}, which was reached approximately after 350 s in all cases and maintained for t_{ss} = 300 s. Concerning the laser power, it is maintained constant for the first seconds of the procedure. Then it suddenly changes to 5 W. For d = 6.0 mm and 7.2 mm, 5 W are maintained for ~100 s, whereas for d=10.8 mm it is maintained for ~200 s. After this constant phase, the power decreases until to reach another plateau at approximately 2 W. This plateau corresponds to the constant and desired temperature profile measured in the tissue, and achieved with the implemented control strategy.

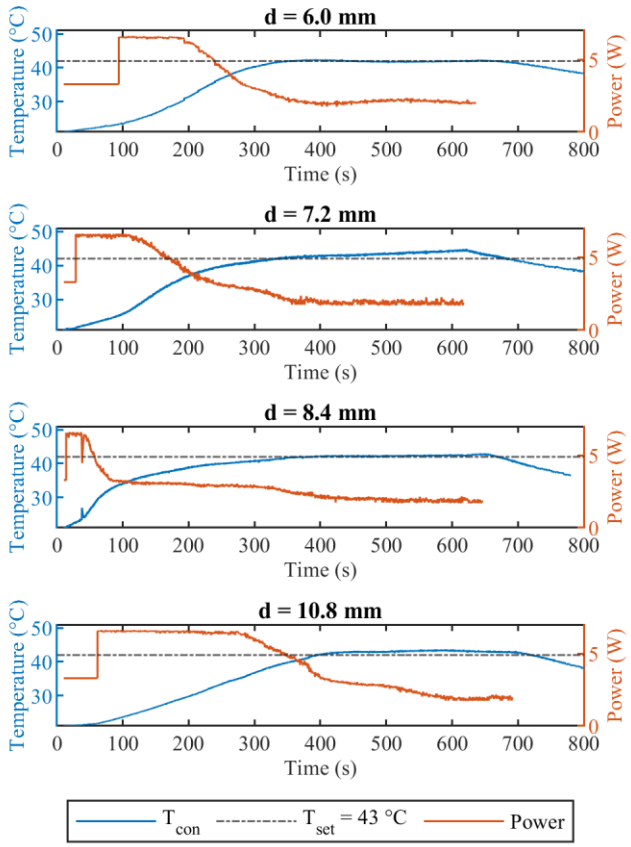

Fig. 6. Measured controlled temperature, set temperature (43 °C) and laser power profiles for different controlled distances.

Fig. 7 illustrates controlled temperatures for different d values and related maximum measured temperatures (dashed lines). Despite the high differences between controlled and maximum temperatures (up to 140 °C), the control has an overdamped behavior for all tests. The results shown in this figure further highlight the key-role of the implemented control strategy for the application. Indeed, the complexity of the pancreas structure from the biological, optical and thermal points of view causes irregular heat-transfer in the organs, as demonstrated by the high and irregular maximum temperature profile measured by on the FBGs of the array. Thus, the absence

of a suitable control strategy can worsen the performance of the LA procedure.

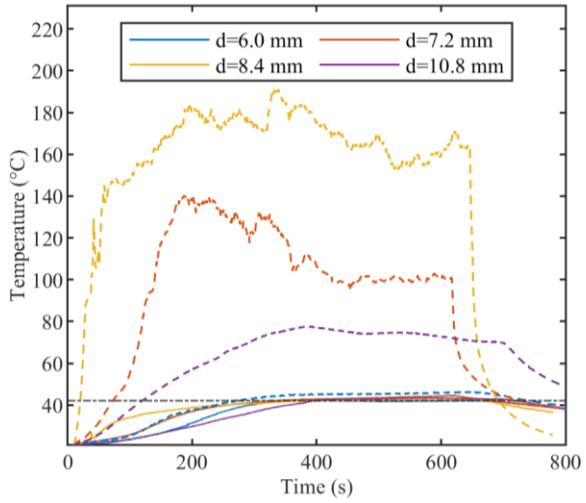

Fig. 7. Measured controlled temperature profiles (solid lines) and maximum measured temperature profiles (dashed lines) for different controlled distances.

The high spatial resolution of the highly dense FBG arrays allows for reconstructing temperature evolution maps (distance along the array *vs.* time) from the measured values, as shown in Fig. 8. The contour maps measured by FBG array during laser ablation are depicted considering relevant temperatures for the LA biological outcome, i.e., 43 °C, 60 °C, and 100 °C. The red line shows the position of the FBG measuring the maximum temperature, and the white line depicts the position of the controlled grating. As can be seen from Fig.9, the set temperature (43 °C contour) does not exceed the defined controlled distance (white line) for all tests. In addition, temperature contours can be used for the evaluation of instantaneous thermal damage ($T \geq 60$ °C) and vapor diffusion and tissue desiccation ($T \geq 100$ °C). We observe that for d=6.0 mm, the FBG array experiences a temperature evolution which is maintained below 60 °C. This result is expected, since the short control distance (with set temperature of 43 °C) does not allow proper heat transfer in the tissue. For d=7.2 mm, d=8.4 mm and d=10.8 mm, the temperature is higher than the case of d=6.0 mm, and at d=10.8 mm, no contour at 100 °C is present. This result is also acceptable, because that the aim of the developed algorithm is to maintain stable temperature at the controlled grating (white line in Fig.8), while the maximum temperature can reach any value depending on laser-tissue interaction (as also shown in Fig. 7).

Fig. 9 shows the repeatability of the temperature control achievable with our approach. In this case, we report the maximum temperature profiles measured by the FBGs (dashed lines) and the controlled temperature measured by the FBG placed at d = 10.8 mm (continuous line). Three trials on different parts of *ex vivo* pancreatic tissue have been repeated, avoiding any overlap of the damaged zone between consecutive tests. As it can be seen, the control algorithm is able to maintain stable temperature during t_{ss} for all trials. The slight differences can be due to the inhomogeneity of the tissue.

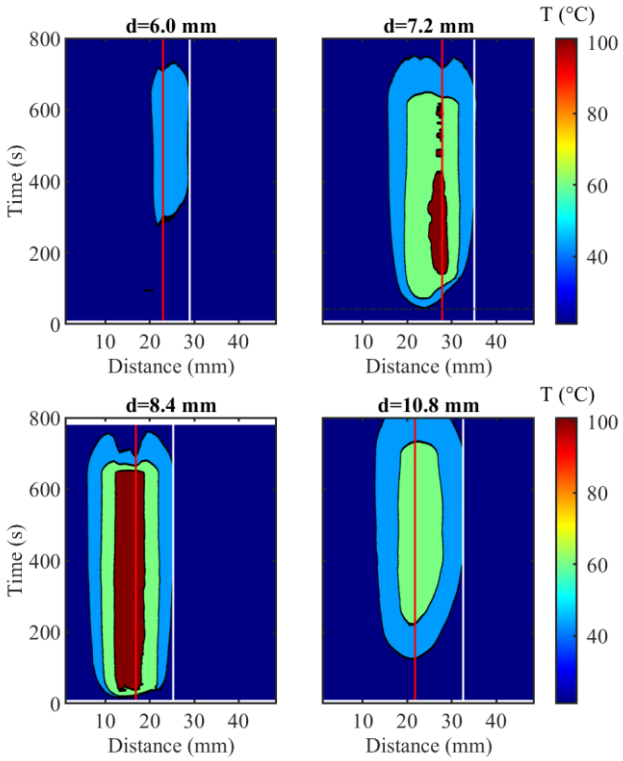

Fig. 8. Measured contour maps during laser ablation with different controlled distances for temperatures: 10 °C, 43 °C, 60 °C, and 100 °C. The red line shows the position of the FBG measuring the maximum temperature, and the white line depicts the position of the controlled grating.

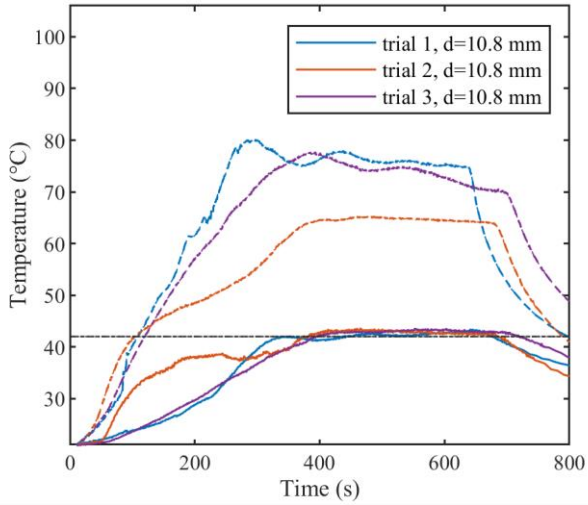

Fig. 9. Measured set temperature profiles (solid lines) and maximum temperature profiles (dashed lines) for the controlled distance of 10.8 mm.

This article has been accepted for publication in a future issue of this journal, but has not been fully edited. Content may change prior to final publication. Citation information: DOI 10.1109/TIM.2021.3112790, IEEE Transactions on Instrumentation and Measurement

Moreover, the high spatial resolution of the sensors can provide information about the thermal gradient. For instance, we observed that across an intra-grating distance of about 2.4 mm, a temperature difference of ~10 °C can be measured (Fig. 10), which proves the need of high-resolution sensors for such measurements.

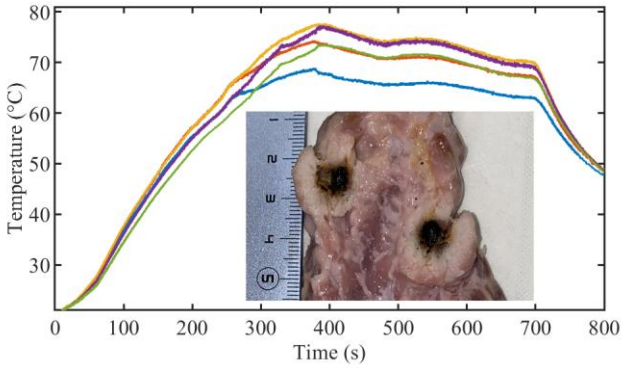

Fig. 10. Measured maximum temperature profile and profiles measured by adjacent gratings for controlled distance of 10.8 mm. The insets shows the resulted ablated region of pancreatic tissue

The final results of LA control are presented in Table II. The energy of the treatment was calculated by using the laser power values used for PID control and the duration of the controlled ablation. Table 2 reports that the size of the ablated area mostly depends on controlled distance *d*, and is less correlated with energy or time of ablation. As a result, the proposed LA regulation approach allows controlling the size of the ablated region by changing the controlled distance parameter.

TABLE II
LA REGULATION RESULTS FOR DIFFERENT CONTROLLED DISTANCES

d (mm)	Time of PID regulation (s)	Energy (J)	Ablated dimensions (mm x mm)
6.0	541.7	1844	7.57 × 6.71
7.2	588.6	1943	12.07 × 8.03
8.4	631.8	1729	14.15 × 10.76
10.8	629.8	2695	17.39 × 14.11

The obtained experimental results validate the proposed PID approach for LA regulation and show the efficacy of FEM-based pre-experiment simulations to obtain effective PID gain values. However, limitations regarding the reliability of the simulations in the prediction of the final clinical outcome are represented by the lack of literature about the behavior of the thermo-optical pancreatic properties with respect to temperatures and by the complexity of photothermal-induced heat transfer in biological tissue. Thus, thermo-optical tissue properties need to be investigated in detail to improve TA simulations and their applications in tumor treatment.

In the proposed approach, temperature measurements performed by custom-made highly dense FBG arrays allow for efficient controlling of temperature at different distances and ablation volumes. The high spatial resolution and electromagnetic immunity of the used sensors provide unique advantages in comparison to traditional measurement techniques. Indeed, in the recent work focused on the PID regulation of LA based on thermocouple measurements, a 0.5 mm plastic plate was positioned between the laser applicator and the thermocouple to prevent laser light artifacts along with self-heating [30]. This approach significantly limits possible clinical applications of all of the standard temperature sensors for LA. For instance, the recent work of Paiella *et al*. on clinical testing of immune-stimulating interstitial laser thermotherapy of the pancreas using a feedback mode with conventional sensors (thermistors) reports unsatisfactory results in terms of device handling, safety, and feasibility [32].

Thus, the limitations of convenient sensors observed in the literature encourage further investigation of fiber optic use for LA control. Indeed, recent investigations of single FBG based measurements for PID-based control were performed for a laser-heated needle for biopsy tract ablation and showed promising results [33], [34]. Also, the use of highly dense FBG arrays for LA regulation has been discussed in the recent works of our group [18]–[20], where an ON-OFF control law yielded undesirable overshoots and delayed responses in the temperature regulation.

Nevertheless, one of the limitations of FBG array use for TA is the temperature-strain cross-sensitivity that can lead to measurement artifacts during temperature monitoring. In our experimental setup, this artifact was minimized using the difference between diameters of the needle utilized for FBG placing (21 G = 0.819 mm) and the FBG array diameter (145 μm). This difference results in slightly looser adhesion between tissue and the sensor, thus decreasing strain effect [35], [36].

In order to significantly reduce strain artifacts stemming from the axial strain and bending, a suitable embodiment (glass or PTFE capillary) to encapsulate FBG needs to be developed. However, it can affect sensor dynamic response and absorb the part of the laser light during LA. As a result, more investigations need to be performed in the encapsulation development to completely avoid strain artifacts during FBG temperature measurements.

IV. CONCLUSION

In conclusion, a temperature-based feedback approach for LA regulation was investigated. For temperature measurements, custom-made highly dense FBG arrays were inscribed in single-core fiber using point-by-point writing technology. The high spatial resolution (1.2 mm) and temperature resistance above the typical maximum temperatures of LA provide unique advantages for thermometry. Moreover, FEM-based iterative simulations were developed to optimize the choice of PID gains. In order to validate the closed-loop approach, the point temperature was controlled at different distances from the laser fiber tip (6 mm, 7.2 mm, 8.4 mm, and 10.8mm). The approach here proposed is an innovative feature for the specific application of laser ablation for tumor treatment, where usually no control at all is performed, but the procedure relies only on the experience of the doctor. The results show effective temperature control for

all distances and for all experimental trials. The results of the work encourage further investigation of FBG array applications for LA regulation.

ACKNOWLEDGMENT

This project has received funding from the European Research Council (ERC) under the European Union's Horizon 2020 research and innovation programme (Grant agreement No. 759159). The work of A.W. and A.D. is supported by the Russian Ministry of Science and Higher Education (Grant No. 14.Y26.31.0017).

REFERENCES

[1] R. L. Siegel, K. D. Miller, and A. Jemal, "Cancer statistics, 2020," *CA. Cancer J. Clin.*, vol. 70, no. 1, pp. 7–30, Jan. 2020, doi: 10.3322/caac.21590.

[2] L. Rahib, B. D. Smith, R. Aizenberg, A. B. Rosenzweig, J. M. Fleshman, and L. M. Matrisian, "Projecting cancer incidence and deaths to 2030: the unexpected burden of thyroid, liver, and pancreas cancers in the United States," *Cancer Res.*, vol. 74, no. 11, pp. 2913–2921, 2014.

[3] J. Han and K. J. Chang, "Endoscopic Ultrasound-Guided Direct Intervention for Solid Pancreatic Tumors.," *Clin. Endosc.*, vol. 50, no. 2, pp. 126–137, Mar. 2017, doi: 10.5946/ce.2017.034.

[4] A. Ruarus, L. Vroomen, R. Puijk, H. Scheffer, and M. Meijerink, "Locally advanced pancreatic cancer: a review of local ablative therapies," *Cancers (Basel).*, vol. 10, no. 1, p. 16, 2018.

[5] E. Schena, P. Saccomandi, and Y. Fong, "Laser Ablation for Cancer: Past, Present and Future," *J. Funct. Biomater.*, 2017, doi: 10.3390/jfb8020019.

[6] L. Bianchi *et al.*, "Thermal analysis of laser irradiation-gold nanorod combinations at 808 nm, 940 nm, 975 nm and 1064 nm wavelengths in breast cancer model," *Int. J. Hyperth.*, vol. 38, no. 1, pp. 1099–1110, 2021.

[7] K. F. Chu and D. E. Dupuy, "Thermal ablation of tumours: biological mechanisms and advances in therapy," *Nat. Rev. Cancer*, vol. 14, no. 3, p. 199, 2014.

[8] A. J. Welch and M. J. C. Van Gemert, *Optical-Thermal Response of Laser-Irradiated Tissue*. Dordrecht: Springer Netherlands, 2011.

[9] P. S. Yarmolenko *et al.*, "Thresholds for thermal damage to normal tissues: an update.," *Int. J. Hyperthermia*, vol. 27, no. 4, pp. 320–43, Jun. 2011, doi: 10.3109/02656736.2010.534527.

[10] J. T. Lin, Y. S. Chiang, G. H. Lin, H. Lee, and H. W. Liu, "In vitro photothermal destruction of cancer cells using gold nanorods and pulsed-train near-infrared laser," *J. Nanomater.*, vol. 2012, 2012, doi: 10.1155/2012/861385.

[11] J. Lin, Y. Hong, and C. Chang, "Selective cancer therapy via IR-laser-excited gold nanorods," Feb. 2010, vol. 7562, p. 75620R, doi: 10.1117/12.841348.

[12] K. Ivarsson, J. Olsrud, and C. Sturesson, "Feedback Interstitial Diode Laser (805 nm) Thermotherapy System : Ex Vivo Evaluation and Mathematical Modeling With One and Four-Fibers," vol. 96, no. September 1997, pp. 86–96, 1998.

[13] P. H. Möller, L. Lindberg, P. H. Henriksson, B. R. Persson, and K. G. Tranberg, "Temperature control and light penetration in a feedback interstitial laser thermotherapy system.," *Int. J. Hyperthermia*, vol. 12, no. 1, pp. 49–63, 1996, doi: 10.3109/02656739609023689.

[14] P. Saccomandi, E. Schena, and S. Silvestri, "Techniques for temperature monitoring during laser-induced thermotherapy: An overview," *Int. J. Hyperth.*, vol. 29, no. 7, pp. 609–619, Nov. 2013, doi: 10.3109/02656736.2013.832411.

[15] F. Manns, P. J. Milne, X. Gonzalez-Cirre, D. B. Denham, J. Parel, and D. S. Robinson, "In situ temperature measurements with thermocouple probes during laser interstitial thermotherapy (LITT): quantification and correction of a measurement artifact," *Lasers Surg. Med. Off. J. Am. Soc. Laser Med. Surg.*, vol. 23, no. 2, pp. 94–103, 1998.

[16] A. Othonos, K. Kalli, and G. E. Kohnke, "Fiber Bragg gratings: Fundamentals and applications in telecommunications and sensing," *Phys. Today*, vol. 53, no. 5, p. 61, 2000.

[17] E. Udd and W. B. Spillman Jr, *Fiber optic sensors: an introduction for engineers and scientists*. John Wiley & Sons, 2011.

[18] S. Korganbayev, R. Pini, A. Orrico, A. Wolf, A. Dostovalov, and P. Saccomandi, "Towards temperature-controlled laser ablation based on fiber Bragg grating array temperature measurements," in *2020 IEEE International Workshop on Metrology for Industry 4.0 & IoT*, 2020, pp. 268–272.

[19] S. Korganbayev *et al.*, "Closed-Loop Temperature Control Based on Fiber Bragg Grating Sensors for Laser Ablation of Hepatic Tissue," *Sensors*, vol. 20, no. 22, p. 6496, 2020.

[20] L. Bianchi, S. Korganbayev, A. Orrico, M. De Landro, and P. Saccomandi, "Quasi-distributed fiber optic sensor-based control system for interstitial laser ablation of tissue: theoretical and experimental investigations," *Biomed. Opt. Express*, vol. 12, no. 5, p. 2841, May 2021, doi: 10.1364/BOE.419541.

[21] T. Erdogan, "Fiber grating spectra," *J. Light. Technol.*, vol. 15, no. 8, pp. 1277–1294, 1997.

[22] K. T. V Gratten and B. T. Meggitt, *Optical Fiber Sensor Technology*, vol. 3. Boston, MA: Springer US, 1999.

[23] L. Huang, R. S. Dyer, R. J. Lago, A. A. Stolov, and J. Li, "Mechanical properties of polyimide coated optical fibers at elevated temperatures," in *Optical Fibers and Sensors for Medical Diagnostics and Treatment Applications XVI*, Mar. 2016, p. 97020Y, doi: 10.1117/12.2210957.

[24] A. V Dostovalov, A. A. Wolf, A. V Parygin, V. E. Zyubin, and S. A. Babin, "Femtosecond point-by-point inscription of Bragg gratings by drawing a coated fiber through ferrule," *Opt. Express*, vol. 24, no. 15, pp. 16232–16237, 2016.

[25] P. Saccomandi, A. Lapergola, F. Longo, E. Schena, and G. Quero, "Thermal ablation of pancreatic cancer: A systematic literature review of clinical practice and pre-clinical studies," *Int. J. Hyperth.*, vol. 35, no. 1, pp. 398–418, Dec. 2018, doi: 10.1080/02656736.2018.1506165.

[26] M. H. Niemz, *Laser-tissue interactions*. Springer, 2007.

[27] P. Saccomandi *et al.*, "Theoretical Analysis and Experimental Evaluation of Laser-Induced Interstitial Thermotherapy in Ex Vivo Porcine Pancreas," *IEEE Trans. Biomed. Eng.*, vol. 59, no. 10, pp. 2958–2964, Oct. 2012, doi: 10.1109/TBME.2012.2210895.

[28] T. H. Nguyen, Y. Rhee, J. Ahn, and H. W. Kang, "Circumferential irradiation for interstitial coagulation of urethral stricture," *Opt. Express*, vol. 23, no. 16, pp. 20829–20840, 2015.

[29] A. Ishimaru, "Diffusion of light in turbid material," *Appl. Opt.*, 1989, doi: 10.1364/ao.28.002210.

[30] T. H. Nguyen, S. Park, K. K. Hlaing, and H. W. Kang, "Temperature feedback-controlled photothermal treatment with diffusing applicator: theoretical and experimental evaluations," *Biomed. Opt. Express*, vol. 7, no. 5, p. 1932, May 2016, doi: 10.1364/BOE.7.001932.

[31] A. J. Welch and M. J. C. Van Gemert, *Optical-Thermal Response of Laser-Irradiated Tissue*, vol. 2. Dordrecht: Springer Netherlands, 2011.

[32] S. Paiella *et al.*, "Laser Treatment of Pancreatic Cancer with Immunostimulating Interstitial Laser Thermotherapy Protocol: Safety and Feasibility Results From Two Phase 2a Studies," *J. Surg. Res.*, vol. 259, pp. 1–7, 2021.

[33] H. H. Abd Raziff *et al.*, "A Temperature-Controlled Laser Hot Needle with Grating Sensor for Liver Tissue Tract Ablation," *IEEE Trans. Instrum. Meas.*, vol. 69, no. 9, pp. 7119–7124, 2020, doi: 10.1109/TIM.2020.2978920.

[34] H. H. A. Raziff *et al.*, "Laser-heated needle for biopsy tract ablation: In vivo study of rabbit liver biopsy," *Phys. Medica*, vol. 82, no. February, pp. 40–45, 2021, doi: 10.1016/j.ejmp.2021.01.067.

[35] L. Bianchi *et al.*, "Fiber Bragg Grating Sensors-based Thermometry of Gold Nanorod-enhanced Photothermal Therapy in Tumor Model," 2021.

[36] B. A. Patterson, D. D. Sampson, P. A. Krug, and S. K. Jones, "In vivo quasi-distributed temperature sensing with fibre Bragg gratings," in *Technical Digest. Summaries of papers presented at the Conference on Lasers and Electro-Optics. Postconference Technical Digest (IEEE Cat. No. 01CH37170)*, 2001, pp. 402–403.

Sanzhar Korganbayev (Student Member, IEEE) received the B.S. and M.S. degrees in electrical and electronics engineering from Nazarbayev University, Nur-Sultan, Kazakhstan, in 2016 and 2018, respectively. He is currently pursuing a Ph.D. degree with the Department of Mechanical Engineering, Politecnico di Milano. He is currently involved in the "LASER OPTIMAL" Project (European Research Council Grant GA 759159) for the development of software for real-time temperature monitoring and intra-operative adjustment of the laser ablation settings during tumor treatment. His research interests include fiber optic sensors and their applications for thermal and mechanical measurements.

Annalisa Orrico (Student Member, IEEE) received the B.S. and M.S. degrees in mechanical engineering from Politecnico di Milano, in 2017 and 2020, respectively. She is currently pursuing a Ph.D. degree with the Department of Mechanical Engineering, Politecnico di Milano. She is currently involved in the "HyperSIGHT" project (ID R18SF4YHHS) for the development of spectral imaging based tools for the monitoring and the prediction of thermal effects on tissues. Her other research interest is the application of fiber optic sensors for thermal measurements.

Leonardo Bianchi (Student Member, IEEE) received the M.Sc. degree (*cum laude*) in Biomedical Engineering from Politecnico di Milano, in 2019. Currently, he is a Ph.D. student at the Department of Mechanical Engineering of Politecnico di Milano, where he is working in the framework of the "LASER OPTIMAL" project (European Research Council Grant - GA 759159). His research interests include the optimization of tumor laser ablation, from both the numerical modeling and experimental assessment, nanoparticle-assisted photothermal therapies, and the related sensing techniques for temperature monitoring during treatments.

Davide Paloschi (Student Member, IEEE) received the B.S. and M.S. degrees in Automation and Control Engineering from Politecnico di Milano, Milan, Italy, in 2016 and 2018, respectively. From 2019 to 2020, he has been a Research Fellow at Politecnico di Milano in the department of Mechanical Engineering. He is currently a Ph.D. candidate in the same department. His main research interest regards the monitoring of physiological parameters. His other research interests are model prediction, data analysis and noise filtering.

Alexey Wolf received an M.Sc. degree in Physics from Novosibirsk State University (NSU) and a Ph.D. degree in Optics from the Institute of Automation and Electrometry of the SB RAS (IAE SB RAS) in 2013 and 2020, respectively. He currently works as a researcher in the Laboratory of Nonlinear Waveguide Systems at NSU and the Laboratory of Fiber Optics at IAE SB RAS, where he develops new types of fiber lasers and sensors based on specialty optical fibers. His scientific interests include femtosecond laser micromachining, fiber Bragg gratings, and new optical materials.

Alexander Dostovalov received an M.Sc. degree in Physics from Novosibirsk State University (NSU) and PhD degree in Optics from the Institute of Automation and Electrometry of the SB RAS (IAE SB RAS) in 2009 and 2015, respectively. Since 2018, he has been a senior research fellow with Institute of Automation and Electrometry and the Laboratory of Nonlinear Waveguide Systems at NSU. He is the author of more than 35 articles and 5 inventions. His research interests include femtosecond laser micromachining, fiber Bragg gratings inscription, fiber lasers and sensors.

Paola Saccomandi (Senior Member IEEE) received her Ph.D. in Biomedical Engineering from Università Campus Bio-Medico di Roma in 2014. From 2016 to 2018 she was a postdoctoral researcher at the IHU - Institute of Image-Guided Surgery of Strasbourg. Since 2018 she is an Associate Professor at the Department of Mechanical Engineering of Politecnico di Milano. She is the Principal Investigator of the European Research Council grant "LASER OPTIMAL"- GA 759159. The main research interests of Prof. Saccomandi and her team include fiber optic sensors, biomedical imaging, and the development of light-based approaches for hyperthermal tumor treatment and monitoring.